

An Optimal Energy Efficient Design of Artificial Noise for Preventing Power Leakage based Side-Channel Attacks

Shan Jin, Minghua Xu, Riccardo Bettati, and Mihai Christodorescu

Abstract—Side-channel attacks (SCAs), which infer secret information (for example secret keys) by exploiting information that leaks from the implementation (such as power consumption), have been shown to be a non-negligible threat to modern cryptographic implementations and devices in recent years. Hence, how to prevent side-channel attacks on cryptographic devices has become an important problem. One of the widely used countermeasures to against power SCAs is the injection of random noise sequences into the raw leakage traces. However, the indiscriminate injection of random noise can lead to significant increases in energy consumption in device, and ways must be found to reduce the amount of energy in noise generation while keeping the side-channel invisible. In this paper, we propose an optimal energy efficient design for artificial noise generation to prevent side-channel attacks. This approach exploits the sparsity among the leakage traces. We model the side-channel as a communication channel, which allows us to use channel capacity to measure the mutual information between the secret and the leakage traces. For a given energy budget in the noise generation, we obtain the optimal design of the artificial noise injection by solving the side-channel’s channel capacity minimization problem. The experimental results also validate the effectiveness of our proposed scheme.

Index Terms—Side-Channel Attacks, Artificial Noise, Energy Efficiency, Channel Capacity

I. INTRODUCTION

A. Background

Side-channel attacks (SCAs), which exploit physical information that leaks from the target devices to extract secret information (keys, password, etc.), have shown to be successful in breaking a large number of cryptographic algorithms, implementations, or security in general over the years. The effectiveness of side-channel attacks is based on the fact that the physical information leakages are dependent on the internal state (secret) of the device. This dependency is often called *leakage model* or *leakage function* [1]. There is a variety of forms of physical leakages, such as electromagnetic emanation [2], acoustic emanation [3], power consumption [4], or others. As IoT (Internet of Things) and embedded devices in general are easily physically accessible, they are highly vulnerable to these forms of physical side-channel attacks.

Shan Jin and Minghua Xu are with Visa Research, Austin, TX, 78759. (e-mail: shajin@visa.com, mixu@visa.com)

Riccardo Bettati is with Texas A&M University, College Station, TX, 77843. (e-mail: bettati@tamu.edu)

Mihai Christodorescu is with Google LLC, Mountain View, CA, 94043. (e-mail: christodorescu@google.com)

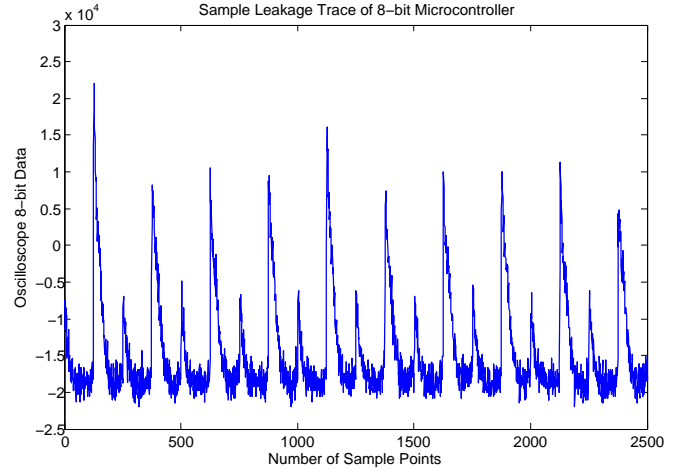


Fig. 1: Sample of a Power Trace (Derived from the Dataset in [5])

Power consumption analysis is a widely studied method for side-channel attacks. By analyzing the power consumed by a particular device during a computation, attackers attempt to infer the secret inside the device. Fig. 1 shows an example of the power consumption, in this case, the current is drawn from a 8-bit micro-controller [5]. In the following of this paper, we will focus on power consumption based side-channel attacks.

Fundamentally, side-channel attacks can be distinguished as non-profiled and profiled attacks. In *non-profiled* side-channel attacks, the attacker leverages an *a-priori* assumption about the leakage model for extracting the secret. In power consumption based side-channel attacks, there are two widely used models in non-profiled attacks: The *Hamming Weight* (HW) model [1], which assumes the power consumption depends on the number of “ones” in the secret, and the *Hamming Distance* (HD) model [6], which assumes that the power consumption depends on the number of bit flips between two consecutive internal states.

In *profiled* side-channel attacks, the attacker first collects the leakage traces from the identical or from a similar device, and then learns the leakage model based on the collected data. This renders profiled side-channel attacks to be data-driven approaches. There are two commonly used techniques in profiled attacks, which are the *Template Attack* [7], [8] and the *Stochastic Model* [9]. In the Template Attack, the attacker builds for each secret key a separate model, which is called

a *template*. The template typically is in form of Gaussian Model. During the attack, the attacker extracts the key by selecting that candidate key whose template best matches the leakage traces collected during the attacking phase [10]. In the Stochastic Model, each time-sample point of the leakage trace is modeled as a linear combination of a secret (in binary string) and a coefficient vector, to which an independent noise is added. Hence, now profiling a leakage model is equivalent to estimating the coefficients at each time-sample point.

B. Related Work

As the security in cryptographic devices and implementations has always been a top priority, how to prevent side-channel attacks on these devices is an important question for system designers. As we mentioned, the effectiveness of side-channel attacks is based on the fact that the physical leakage traces are dependent on the secret. Hence, breaking this dependency is an intuitive way to counter side-channel attacks. There are two methods that have been discussed in the literature: Masking [11], and random noise generation [12].

Masking acts directly at the algorithmic level of the cryptographic implementation. The principle of this technique is to randomly split the secret into multiple (for example $d + 1$) *shares*, where any d shares can not reveal the sensitive information. The authors in [11] proved that, given the leakage on each share, the bias of the secret decreases exponentially with the order of d . Recent research on code-based Masking [13] further enhances the side-channel security. However, although masking is shown to be an effective countermeasure to side-channel attacks, it requires a complete re-design or reconstruction of the cryptographic implementation, such as the masked S-Box in AES Masking [14], which is quite invasive to the design process. The redesign of the algorithmic modules is costly and excludes the possibility of directly using current standard IP blocks.

Different to masking, random noise generation based method does not directly work on the core architecture of the cryptographic implementation [12]. Typically, the generation of the noise sequences is independent to the cryptographic operations. By superposing the random noises on the raw leakage traces, the SNR (signal-to-noise ratio) of the leakage signal received by the attacker is decreased, which eventually hides the power consumption leakage of the secret-dependent operation. However, as shown in [15], this technique is not energy efficient, as it incurs a huge overhead (nearly 4 times the AES current consumption) in order to obtain a high resistance to CPA (Correlation Power Analysis) [1] based attack. But, this energy consumption can be reduced by one simple observation: from [8], we noticed that only a few samples in leakage traces contain useful information that relate to the secret in the target device. This gives us an idea for designing more energy efficient approach to generate the artificial noise to prevent side-channel attacks.

Besides, previous work in [16], [17] has also focused on the issue of preventing side-channel attacks based on voltage regulation. The key idea of these work is to embed protection on the voltage regulator, and hence degrade the

SNR of the power traces that used in attack. Although the effectiveness of the protection in these work is recognized, one of the limitations is they both indiscriminately compensate the entire large-signal power, which bring the same problem of costly energy consumption in defending against the side-channel attacks as the random noise generation. Recently, the work in [18] proposed a machine learning based approach to compensate the small signal power, which considered the issue of power overhead reduction. However, this approach relied on the applying of the supervised machine learning, which brings a new issue of the cost in the implementation, especially to the small-sized IoT (internet of things) devices.

C. Contributions

In this paper, we present an energy efficient design of artificial noise to prevent power consumption based side-channel attacks. First, we map the side-channel attacks model to a traditional communication model. As we notice, from the view of the secret communication [19], the attackers in side-channel attacks play the same role as that of eavesdroppers in a communication model, and the side-channel is equivalent to the eavesdropper's channel. Hence, similarity to the case of secret communication, where the transmitter generates the artificial noise to degrade the eavesdropper's channel, in this paper we also design a scheme to generate artificial noise on the device to degrade the side-channel for preventing side-channel attacks.

Besides, different from previous random noise generation based methods, our approach exploits the sparsity among the leakage traces to generate the artificial impulsive noise sequence. Since the mutual information between the side-channel leakage and the secret can be modeled as a channel capacity, our design aims at minimizing the channel capacity under a given energy constraint on the generation of the artificial noise sequences. As a result, our solution achieves what we call *optimal energy efficiency* (EE) while maintaining the protection to against the side-channel attacks.

Furthermore, compared to the work in [18], our approach does not use the supervised machine learning. Instead, we derive an optimal structure of modulator, which is used to regulate an impulse signal generator to maximize the protection for the target device. Our method is simpler to implement and also friendly to deploy compared to the machine learning approach, and would be more cost effective for small-sized IoT devices. In addition, our solution is controllable in terms of trade-off between using more energy to achieve strong protection and using just modest energy for a satisfactory protection.

D. Paper Organization

The remaining part of this paper is organized as follows. Section II introduces the system model. The data compression is discussed in Section III. The optimal energy efficient design is introduced in Section IV. The further discussion on the designed scheme is given in Section V. Section VI presents the experimental results. The paper is concluded in Section VII.

II. SYSTEM MODEL

A. Modeling Side Channels as Communication Channels

A variety of previous work has focused on the problem of mapping side-channel attacks model to communication models. In [20], a general uniform framework is proposed to integrate side-channel attacks and classic communication theory. Under this framework, the effect of the modeled leakage function can be quantified. In [21], by viewing the side-channel as a noisy channel in communication theory, the authors designed a number of optimal side-channel distinguishers for different scenarios. In [22], the authors model the side-channel as a fading channel. As a result, the profiling problem in side-channel attacks can be formulated as a channel estimation problem in communication systems.

Generally, the side-channel model can be modeled as:

$$L = Y(X) + N, \quad (1)$$

where $L \in \mathbb{R}^{m \times 1}$ is the leakage trace, X is the internal state (secret) in the implementation, $Y(X) \in \mathbb{R}^{m \times 1}$ is the deterministic part of the side-channel leakage, which is dependent on X , and $N \in \mathbb{R}^{m \times 1}$ is the random part and typically is modeled as an i.i.d Gaussian noise vector with distribution $\mathcal{N}(\mu_N, \Sigma_N)$.

Typically, there are two widely used models to represent the side-channel leakage, in non-profiled and profiled side-channel attacks, respectively:

a) *Hamming Weight Model*: In non-profiled side-channel attacks, the side-channel leakage is assumed to follow a Hamming Weight (HW) model, which is represented by:

$$L = \text{HW}(X) + N, \quad (2)$$

where $\text{HW}(\cdot)$ is the Hamming Weight function. A special case of HW model is the Hamming Distance (HD) model, where the power leakage is dependent on the HD function of the internal state, which is the result of XOR operation between the states before and after the cryptographic operations.

b) *Linear Model*: Previous work, especially the Stochastic Model [9], has shown that the side channel can be linearly represented [22]. Suppose the binary string vector of the secret X is $F_b(X) \in \mathbb{R}^{(B+1) \times 1}$ where B is the number of the bits and $\text{bit}_b(X)$ is defined as the b -th bit value of the binary string (typically $\text{bit}_0(X) = 1$ is assumed), and $W \in \mathbb{R}^{m \times (B+1)}$ is the leakage coefficients matrix where each element w_{ij} is the weight coefficient at sample point i for the leakage caused by bit $j + 1$, there is a linear relationship between L and X :

$$L = W F_b(X) + N. \quad (3)$$

Linear model is typically used in profiled side-channel attacks, where the leakage matrix (model) W is built in the profiling phase and used in attack phase.

Generally, beyond which type of leakage model is applied, in traditional information theory, a common metric to measure how much information of secret X that contained in the leakage trace L is the *mutual information* [20], [23], which is defined as:

$$I(L; X) = H(X) - H(X|L), \quad (4)$$

where $H(X)$ is the entropy of X and $H(X|L)$ is the conditional entropy of X based on L .

The maximum mutual information leaked through a side-channel is typically called *channel capacity* [24], which is expressed as:

$$C = \max I(L; X). \quad (5)$$

We note that the side-channel attack model differs from the classical communication model: In side-channel attacks, the leakage trace is measured (received) by the attacker. However, rather than acting as the receiver, now the attacker in fact plays the role of the eavesdropper as in the communication model [19]. Hence, the attacker can not influence the input (the target secret X) in the target implementation (transmitter) through the communications between the transmitter and the attacker as in the communication model, and therefore can not optimize the channel capacity of the side-channel.

Previous work in [23] also focused on the same issue, where the authors construct the side-channel's channel capacity by modeling the leakages as MIMO (multi-input multi-output) channels [25]. However, the modeling of the side-channel leakages is not limited to the linear model. On the contrary, a variety of non-linear models have been proposed and fully studied, such as convolutional neural networks [26] and the quadratic model [6]. Hence, in this paper, similarity to the work in [21], we use a general model to characterize the side-channel, where we treat the side-channel as an additive *noisy channel*, as shown in Eq. (1). Hence, now the channel capacity of the side-channel is expressed by [24]:

$$C = \frac{1}{2} \log(1 + \text{SNR}) = \frac{1}{2} \log \left(1 + \frac{|Y(X)|^2}{E[|N|^2]} \right), \quad (6)$$

where $E(\cdot)$ is the expectation function, and SNR is the signal-to-noise ratio of the leakage signal received by attacker. We also note that the channel capacity formula Eq. (6) can be easily applied to all forms of leakage models, such as HW or HD model, the linear model, and any non-linear models, given that $Y(X)$ is the side-channel leakage function part.

B. Generating Noise Sequence to Counter Side-Channel Attacks

As shown in Eq. (6), the mutual information between the secret X and the leakage trace L is decided by the SNR of the received leakage signals. Hence, from the view of the traditional communication theory, mitigating the power of the side-channel attacks is equivalent to reducing the SNR of the leakage signals received by the attacker. In communication model, one way to achieve this SNR reduction is to inject random noise into the transmitted signal. As a result, the SNR of the signal received by the eavesdropper is decreased, which eventually degrades the eavesdropper's channel. This is the basis for jamming [27], [28]. Similarly, in side-channel attacks, it is also shown that injecting random noise on original leakage traces is a practical way to counter side-channel attacks [12], [29].

Fig. 2 shows the system model of general embedded noise generator within the target computing system. The *cryptographic engine* is the core part in the system. It performs the

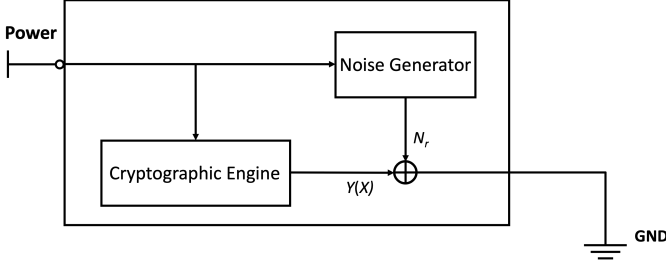


Fig. 2: System Model of General Embedded Noise Generator

cryptographic operations, such as the AES engine in an IoT device. The noise sequence is independently and randomly generated from the *noise generator*, which is then injected into the raw leakage trace that is emitted from the engine during the computation. As a result, the raw leakage trace and the random noise sequence are mixed together, which results in a "new" leakage trace that the attacker only can measure. Generally, the leakage traces superposed by the random noise can be expressed as:

$$\hat{L} = Y(X) + N + N_r, \quad (7)$$

where N_r is the i.i.d random noise vector, with a distribution $\mathcal{N}(\mu_r, \Sigma_r)$. Now the capacity of the side-channel becomes:

$$C = \frac{1}{2} \log(1 + SNR) = \frac{1}{2} \log \left(1 + \frac{|Y(X)|^2}{E[|N_r|^2] + E[|N|^2]} \right), \quad (8)$$

Compared to Eq. (6), the addition of the term $E[|N_r|^2]$ in the denominator decreases the SNR in Eq. (8) as well as the channel capacity.

While the random noise generation method clearly works and is easily to implement, previous work also shows that this method leads to significant energy consumption: In [15], the authors measured that in order to get a high enough resistance to side-channel attacks on AES, the current consumption is increased by a factor of four. This motivates the need to design an energy efficient and also powerful noise generation scheme to counter side-channel attacks.

III. DATA COMPRESSION TECHNOLOGIES

Before we introduce the design of the proposed energy efficient scheme, we need to discuss the compression of the leakage data during the profiling and the attack phases. It has been observed (for example in [7], [8], [30]) that often only very few leakage samples of the raw leakage traces contain useful leakage information. We say that the leakage traces are *sparse*. This sparsity is caused by the fact that many other activities in the implementation of the cryptographic system that are not dependent on the secret, due to fixed I/O (Input/Output) activities. Thus, in order to perform an efficient attack, one has to *compress* the collected leakage traces to extract the useful leakage information. A widely used method to compress the large amount of data is the so-called *sampling selection*: by selecting a subset from all recorded leakage samples, the number of samples is reduced. A variety of methods to select the samples have been developed, such as

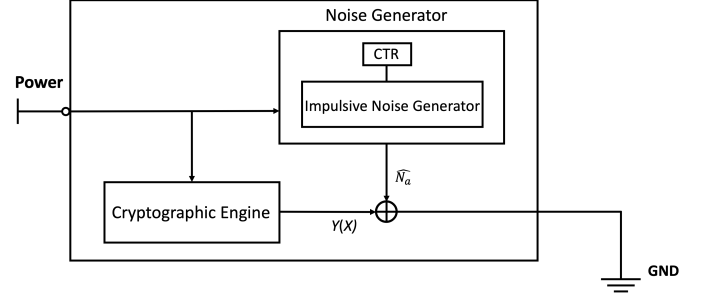


Fig. 3: System Model of Artificial Noise Generator

Difference of Means (DoM) [7] (which includes 1ppc, 3ppc, 20ppc and allap), Sum of Squared Pairwise T-Differences (SOST) [31], or Signal-to-Noise Ratio (SNR) [32].

Generally, the data compression process can be represented as:

$$PL = PY(X) + PN, \quad (9)$$

where $P \in \mathbb{R}^{m_c \times m}$ with $m_c \ll m$ is the *compression matrix*. In the case of sampling selection, the compression matrix is also called the *sampling matrix*. Each row in P has at most one "1", and the index of the "1" in each column of P stands for which sample in the leakage signal $Y(X)$ is to be picked. (We can think of the sampling matrix as a permutation matrix with additional zero columns.). For example, if we consider a sampling process where only the 1st, 2nd, and the last leakage samples are picked (now $m_c = 3$), then P could be expressed by

$$P = \begin{bmatrix} 1 & 0 & 0 & \dots & 0 \\ 0 & 1 & 0 & \dots & 0 \\ 0 & 0 & 0 & \dots & 1 \end{bmatrix}. \quad (10)$$

Note once the sampling method is chosen, P is defined.

IV. OPTIMAL ENERGY EFFICIENT DESIGN

A. Artificial Noise Generation

In this paper, we propose a scheme to prevent side-channel attacks by designing artificial noise sequences, which are then superposed onto the raw leakage trace. The system model of the designed artificial noise generator is shown in Fig. 3.

From the model, the observed leakage trace can therefore be represented as:

$$\hat{L} = Y(X) + N + \hat{N}_a. \quad (11)$$

The term \hat{N}_a is the artificial noise generated from the designed noise generator, which is defined as:

$$\hat{N}_a = \rho F N_a, \quad (12)$$

where ρ is the gain factor, and N_a is i.i.d Gaussian distributed noise with the distribution $\mathcal{N}(\mu_a, \Sigma_a)$. The covariance Σ_a is a diagonal matrix with identical value σ_a in the diagonal.

In the system model, N_a is the noise source of the *impulsive noise generator*, and ρ is the *gain* on the amplitude of the generated impulsive noise. As we mentioned before, random noise generation is not energy efficient as it generates noises

to corrupt all leakage samples. Besides, as introduced in Section III, typically only a subset of leakage samples contain secret-dependent useful information. Hence, our designed noise sequence which aims at only corrupting those useful sample is in fact a *impulsive noise sequence*. Moreover, our noise generator can directly apply the majority modules in the traditional impulsive noise generator [33], but only makes the change on the modeling of the inter-arrival times of the generated noise sequence: Different to the traditional impulsive noise generator, where the inter-arrival times of the impulsive noise is modeled as a *Markov renewal process* (MRP) [33], [34] and hence the inter-arrival time between two consecutive impulses is random (controlled by a Markov state-transition probability matrix), the inter-arrival times of the impulse noise in our noise generator is pre-defined. More specifically, by artificially control the generation of the impulsive noise, we can generate an impulsive noise sequence with a predictive pattern to decide where the impulses are appeared. The inter-arrival times between those impulses are therefore defined. Typically, the generation pattern could be represented by a state-transition probability matrix, and is stored and triggered in the control module **CTR** in the noise generator. The transition matrix is expressed by:

$$G = \begin{bmatrix} \beta_{1,1} & \beta_{1,2} & \dots & \beta_{1,n} \\ \beta_{2,1} & \beta_{2,2} & \vdots & \beta_{2,n} \\ \vdots & \vdots & \ddots & \vdots \\ \beta_{n,1} & \beta_{n,2} & \dots & \beta_{n,n} \end{bmatrix}, \quad (13)$$

where n is the total number of states in the impulsive noise sequence generation, $\beta_{i,j}$ is the transition probability from state s_i to s_j , and the state s_i represents where the i -th impulse event should be occurred in the sequence given the first $i-1$ impulses is pre-defined. Hence n equals the maximum number of the impulses that could be generated in a duration. As we mentioned that the generation of the impulsive noise sequence is pre-defined in our design, we have $\beta_{i,j} = 1$ only if s_i matches with the first i impulses in s_j ($s_i = s_{j-1}$), and $\beta_{i,j} = 0$ for the rest of the cases. In this case, G is in fact a *sparse matrix* since majority of the elements in G is 0.

Actually, the design of the transition matrix can be mapped to a process of impulsive noise samples selection. This selection of the generation of the impulsive noises (which can also be viewed as a set of instructions to trigger the impulsive generation or not) is represented by the diagonal matrix $F \in \mathbb{R}^{m \times m}$, which injects the impulsive noises into a subset of samples of the original leakage trace $Y(X)$. Values on the diagonal can be "0" or "1", and the positions of the "1"s in the diagonal decide which artificial noise samples will be generated and injected into the leakage trace, i.e., for which samples in the leakage trace we inject the impulsive noises. As an example, if the impulsive samples are generated and injected into only the beginning and the end points of a leakage

trace, then F would be:

$$F = \begin{bmatrix} 1 & 0 & \dots & 0 \\ 0 & 0 & \dots & 0 \\ \vdots & \vdots & \ddots & \vdots \\ 0 & 0 & \dots & 1 \end{bmatrix}. \quad (14)$$

In contrast to the indiscriminate random noise generation approach that described in Section II, based on our designed noise generation model, we can exploit the fact of sparsity in leakage trace that the number of useful leakage samples is small as shown in Section III, and only generate a small number of noise samples to inject into the raw leakage trace. This brings the basis for us to design more energy-efficient scheme to generate noise sequence for countering side-channel attacks.

In general, our proposed design takes the following steps: First, given the original device which doesn't have any noise generator attached, the system designer measures the raw leakage traces that are emitted from the cryptographic engine. Then, based on a pre-defined sampling method P , the designer extracts a subset of samples from the raw leakage trace and obtains the parameters that are related to these leakage samples. Typically these device hardware related parameters include the mean, variance, duration, spectra, etc., which will then be used to construct the basic modules of the impulsive noise generator. Besides, based on the sampling method P and other system design requirements (such as the energy constraint on noise generation), the designer constructs a selective process F for generating the impulsive noise sequence, and F will be mapped to construct the state-transition matrix G . As a result, G will be stored as fixed parameters into the CTR. Finally, once the noise generator is constructed, it will be sealed into the system, attached with the cryptographic engine. As we can notice, the key point work is how to design the F in order to generate the optimal energy-efficient artificial noise sequence. We will give more details to discuss this problem in the following sections.

B. Optimizing the Artificial Noise Generation

Assuming that now the leakage trace is perturbed by an artificial noise sequence \widehat{N}_a , and the sample selection sampling matrix P is decided, then after the data compression, the collected leakage trace can be expressed by:

$$P\widehat{L} = PY(X) + PN + P\rho FN_a. \quad (15)$$

Here we let $N_P = PN$. Hence, the SNR of the compressed observed leakage trace is:

$$SNR = \frac{|PY(X)|^2}{\rho^2 E[|PFN_a|^2] + E[|N_P|^2]}, \quad (16)$$

where

$$E[|PFN_a|^2] = E[N_a^T F^T P^T PFN_a] = E[N_a^T F^T \hat{P} FN_a]. \quad (17)$$

We use the notation $(\cdot)^T$ to denote the matrix transpose operation.

Let $\hat{P} = P^T P$, here $\hat{P} \in \mathbb{R}^{m \times m}$ is a diagonal matrix with “0”s and “1”s on the diagonal. The index of each “1” on the diagonal exactly match with the index of the “1” in each column of P . If we still use the P in Eq. (10) as an example, now \hat{P} is:

$$\hat{P} = \begin{bmatrix} 1 & 0 & \dots & 0 \\ 0 & 1 & \dots & 0 \\ \vdots & \vdots & \ddots & \vdots \\ 0 & 0 & \dots & 1 \end{bmatrix} . \quad (18)$$

Then we let $\Delta = F^T \hat{P} F$, based on the matrix trace operation, we have

$$\mathbb{E}[|PFN_a|^2] = \mathbb{E}[\text{Tr}(N_a^T \Delta N_a)] = \text{Tr}(\mathbb{E}[\Delta N_a N_a^T]) . \quad (19)$$

As a result, the channel capacity of the side-channel becomes:

$$C_s = \frac{1}{2} \log \left(1 + \frac{|PY(X)|^2}{\rho^2 \text{Tr}(\mathbb{E}[\Delta N_a N_a^T]) + \mathbb{E}[|N_P|^2]} \right) . \quad (20)$$

From Eq. (20), we see that, for a predefined sampling method P , and a target secret X in the target implementation, the energy of the received compressed signal, $|PY(X)|^2$, is fixed. Since N is specified by the machine, $\mathbb{E}[N_P^2]$ is also fixed for a given implementation device. Hence, in order to maximize the effectiveness in securing the target implementation from side-channel attacks, the objective is to minimize the channel capacity C_s in Eq. (20) by appropriately designing the artificial noise \widehat{N}_a . This is to occur in a way that minimizes the energy spent generating the noise sequence.

In general, as is also noted in [19], in order to guarantee the confidentiality of a secret communication, the artificial noise must be designed to maximally degrade the eavesdropper’s channel. More specifically, the objective in [19] is to generate an artificial noise that maximizes the lower bound on the *secrecy capacity*, which is defined as the difference in mutual information between the transmitter-receiver pair and the transmitter-eavesdropper pair (eavesdropper’s channel), as:

$$\widetilde{C}_{sec} = I_{TR} - I_{TE} , \quad (21)$$

where \widetilde{C}_{sec} is the lower bound on the secrecy capacity, I_{TR} is the mutual information on the transmitter-receiver pair and I_{TE} is the mutual information on the transmitter-eavesdropper pair.

However, we note that side-channel attacks models are different, as there is no receiver as in the communication model, and we therefore don’t have to consider the transmitter-receiver pair. As a result, we can treat the mutual information in the transmitter-receiver pair as a constant value (for example let $I_{TR} = 0$). Hence, from the view of secure communication, *maximizing* the secrecy capacity in side-channel attacks is equivalent to *minimizing* the channel capacity in the transmitter-attacker (eavesdropper) pair, which in fact is the side-channel. Therefore, our objective problem is to identify the noise sequence \widehat{N}_a that can minimize the channel capacity C_s of the side channel such that the energy expended on generating the noise sequence does not exceed a given bound

E_A :

$$\begin{aligned} & \min_{\widehat{N}_a} C_s \\ & \text{s.t. } \mathbb{E}[|\widehat{N}_a|^2] \leq E_A , \end{aligned} \quad (22)$$

As we noticed in Eq. (12), F is used to control the selection of the generation of the artificial impulsive noise. For a pre-defined P , a fixed ρ and a given distribution of N_a , the rank of F decides how many impulsive noise samples will be generated, and so controls the total energy to be spent on the noise generation. Hence, the objective problem in Eq. (22) can be translated into:

$$\begin{aligned} & \min_F C_s \\ & \text{s.t. } \text{Rank}(F) \leq A , \end{aligned} \quad (23)$$

where $\text{Rank}(\cdot)$ is the rank of a given matrix, and A is the constraint on the number of impulse noises that can be generated by the noise generator:

$$A = \frac{mE_A}{\rho^2 \text{Tr}(\mathbb{E}[N_a N_a^T])} . \quad (24)$$

From the optimization problem in Eq. (23), we can easily find that minimizing the channel capacity C_s is equivalent to maximizing the energy of the artificial noise. Hence, we can further translate the problem in Eq. (23) as:

$$\begin{aligned} & \max_F \rho^2 \text{Tr}(\mathbb{E}[\Delta N_a N_a^T]) \\ & \text{s.t. } \text{Rank}(F) \leq A . \end{aligned} \quad (25)$$

C. Solution with Optimal Energy Efficiency

In order to find the solution of the optimization problem in Eq. (25), we first observe the matrix Δ , which is defined earlier to be $F^T \hat{P} F$. We also define the set of indices of “1”s of the pre-defined matrix \hat{P} as $\Omega_{\hat{P}}$.

Suppose now under a given constraint A , there is a matrix F , where the set of the indices of “1”s in F is denoted by Ω_F . We also define the set of the indices of “1”s in Δ as Ω_{Δ} . Due to the special property that both \hat{P} and F are diagonal matrices with only 0 and 1 values in their diagonals, Δ is also a diagonal matrix. Furthermore, we also have

$$\Omega_{\Delta} = \Omega_{\hat{P}} \cap \Omega_F , \quad (26)$$

to be always satisfied.

If we further define matrix $\Phi_a = N_a N_a^T$, with the diagonal elements ϕ_i ($1 \leq i \leq m$), we can rewrite Eq. (25) as follows:

$$\rho^2 \text{Tr}(\mathbb{E}[\Delta N_a N_a^T]) = \rho^2 \sum_{i \in \Omega_{\Delta}} \mathbb{E}[\phi_i^2] = c \rho^2 \theta_a , \quad (27)$$

where $c = |\Omega_{\Delta}|$ is the cardinality of Ω_{Δ} , and $\theta_a = \sigma_a^2 - \mu_a^2$. We can find that the maximization of Eq. (27) relies on c , which is eventually decided by \hat{P} and F (under the constraint of A) from Eq. (26). Hence, we can discuss the solution of Eq. (25) under the following cases, which differ in the level of compression of the observed data:

a) $|\Omega_{\hat{P}}| > A$: In this case, considering the system is sensitive to the energy consumption, such as some small-sized

IoT devices, the number of selected leakage samples exceeds the budget of samples to which we can inject impulsive noise. The energy allowed for noise generation is therefore limited.

Now, the maximum rank that F can obtain is $\text{Rank}(F) = A$. In order to maximize $|\Omega_\Delta|$, it requires that

$$\Omega_F = \Omega_{\hat{P}} \cap \Omega_F, \quad (28)$$

as now $|\Omega_F| = A < |\Omega_{\hat{P}}|$. Based on Eq. (26), we have $|\Omega_\Delta| = A$. Hence, the maximum value for Eq. (27) is

$$\max_F \rho^2 \text{Tr}(\mathbb{E}[\Delta N_a N_a^T]) = A \rho^2 \theta_a, \quad (29)$$

and the corresponding optimum F is:

$$F^* = \{F \mid \Omega_F \subseteq \Omega_{\hat{P}}, |\Omega_F| = A\}, \quad (30)$$

where Ω_F of F is any subset of $\Omega_{\hat{P}}$, with $|\Omega_F| = A$. In order to save the computing cost in the device, we set Ω_F is fixed to a given specific system, once the random choice of a subset is generated.

b) $|\Omega_{\hat{P}}| \leq A$: If now the system is friendly to the energy consumption, in this case the energy budget exceeds the number of selected leakage samples. Hence, the maximum of $|\Omega_\Delta|$ is obtained only if

$$\Omega_{\hat{P}} = \Omega_{\hat{P}} \cap \Omega_F, \quad (31)$$

which means $\Omega_{\hat{P}} \subseteq \Omega_F$ is needed.

Besides, although the maximum rank of F could be obtained is A , we don't have to get to this maximum for F . Actually, based on Eq. (26) and Eq. (31), we only need to have $\Omega_{\hat{P}} = \Omega_F$. Hence, the maximum value for Eq. (27) is

$$\max_F \rho^2 \text{Tr}(\mathbb{E}[\Delta N_a N_a^T]) = |\Omega_{\hat{P}}| \rho^2 \theta_a, \quad (32)$$

and the corresponding optimum solution of F is

$$F^* = \hat{P}. \quad (33)$$

In summary, to solve the optimization problem in Eq. (25), the optimum solution of F is obtained by

$$F^* = \begin{cases} \{F \mid \Omega_F \subseteq \Omega_{\hat{P}}, |\Omega_F| = A\}, & \text{if } |\Omega_{\hat{P}}| > A, \\ \hat{P}, & \text{if } |\Omega_{\hat{P}}| \leq A. \end{cases} \quad (34)$$

Once we obtain the optimal design of F , we can easily translate the F^* to the state-transition matrix G^* : Suppose the diagonal of F^* is represented by F_d^* . Then from $i = 1, 2, \dots, m$, if $F_d^*[i] = 1$, we set $s_i = F_d^*[1 : i]$. Then based on the obtained states, the transition matrix can be reconstructed through Eq. (13).

Eq. (34) gives a theoretical solution for how to design the optimal energy-efficient artificial noise sequence. In order to apply the designed scheme to more practical scenarios, we need to further discuss the questions including how to evaluate the energy efficiency of the proposed scheme and also how to compare its energy efficiency to other schemes, as well as how to handle the case when the system's noise generator and the attacker choose different sampling methods. We will elaborate on these questions in the next section.

V. ANALYSIS OF THE NOISE SEQUENCE GENERATION SCHEME

This section further analyzes the proposed design scheme. We will discuss how we evaluate the energy efficiency of the noise generation methods, and the performance boundary of the design for the real applications.

A. Energy Efficiency

As we design method to generate noise sequences in an energy efficient fashion, we need to be guided by a metric that informs us both of their *effectiveness* and the *efficiency*. The former comes in terms of reduction of the success of the attack, and the second in terms of expended energy. The measure used in this paper, which we call *energy efficiency* (EE), combines effectiveness and efficiency by measuring the reduction of the attack success rate per unit of energy spent to generate the noise. This is expressed by

$$EE = \frac{1 - \text{Successful_Key_Recovery}}{\text{Noise_Energy}}, \quad (35)$$

where *Noise_Energy* is the total energy that is spent in generating the noise sequences during an attack. In other words, this is the sum of the energy of all noise sequences that are injected into the leakage traces that are collected by the attacker. When random noise sequence is generated, we have:

$$\text{Noise_Energy} = \sum_{i=1}^I \mathbb{E}[|N_r^{(i)}|^2]; \quad (36)$$

while in the case of the artificial noise sequences, we have

$$\text{Noise_Energy} = \sum_{i=1}^I \mathbb{E}[|\widehat{N}_a^{(i)}|^2], \quad (37)$$

where $N_r^{(i)}$ (or $\widehat{N}_a^{(i)}$) is the noise sequence that has been added to the i -th leakage trace and I is the total number of leakage traces that collected by the attacker. *Successful_Key_Recovery* is a binary value, which indicates whether the attacker is able to recover the secret value despite the noise sequences. If the attacker recovers the key, the value of EE is zero; otherwise, the larger the value of EE, the less energy has been spent to cause an unsuccessful attack. We will use the Eq. (35) to evaluate the energy efficiency of our proposed scheme and other noise generation based methods. More results about the energy efficiency evaluations will be introduced in the experimental part.

B. Choice of Sampling Methods

Eq. (34) in Section III tells us that the optimal noise generation scheme relies on the sampling method that has been chosen for the system in advance. Moreover, the given solution is optimal only when both the system and the attacker choose the same data sampling method. However, in practice, the sampling method chosen by the system during the design phase is likely different from the sampling method that is later used by the attacker. For example, the system may choose

20ppc to construct the artificial noise generator during the design phase, but the attacker may decide to use 3ppc during profiling and attack. Obviously, the system designer does not know which exact compression method that potential attackers will choose in the future. While in addition, once the noise generator is sealed into the system, the attacker also has no way to guess the sampling method utilized by the system.

In practice, however, all the widely used sampling methods (for example those described in [8] and summarized in Section III) are largely similar. For example, the methods SNR and SOST are actually the same if the variance at each sample point is considered to be independent. Similarly, in the DOM family of sampling methods, the samples selected by each method (1ppc, 3ppc, etc.) share a common support. For example, if we set Ω_1 and Ω_3 as the set of indices of samples that selected from the raw leakage trace by 1ppc and 3ppc respectively, the samples collected from 1ppc are always contained in those collected by 3ppc, that is, $\Omega_1 \subseteq \Omega_3$ always holds. Generally, due to this similarity across all these sampling methods, the solution in Eq. (34) given by any sampling method, is closely related to the solutions given by the other methods, under the same constraint.

The question remains about which sampling method to select. The designer faces a trade-off between the scalability of data compression and the amount of energy to be spent for noise sequence generation. For example, if a high-compression method is chosen by the designer, such as 1ppc, more energy is saved in noise generation, but the noise sequence generated by this method may not cover all the useful sample points that will be picked by the attacker if they choose a weaker compression method, such as 20ppc. Similarly, if the designer chooses a very weak compression scheme, such as allap, the generated noise sequence may well mask the majority of the leakage samples that contain useful information, but more energy will be spent. Hence, how to select an appropriate compression method during system design is fundamentally a trade-off between efficiency (what is the energy budget for artificial noise generation) and effectiveness (what is the level of protection against side-channel attacks do we seek). In Section VI, we will evaluate cases where the system and the attacker choose different sampling methods.

C. Time Delay

From the system design in Section IV, it can be found that the effectiveness of our designed scheme is to generate noise samples to corrupt the useful samples inside the raw leakage trace. Ideally, the noise samples generated by Eq. (34) are expected to be exactly injected into the leakage samples that have the same or approximate timing. However, in practice, due to the likely delay introduced by hardware circuit, sometimes the generated noise sequence may not be exactly matched with the leakage trace, for example, the starting point of two sequences is different. This is also called *asynchronization*. In this paper, we only consider the case where both the cryptographic engine and the noise generator are in a synchronization model. Hence, the solution in Eq. (34) can be viewed as a theoretical boundary for the artificial noise

generation model. It will be an interesting and also a valuable future work to explore how to design the artificial noise under the asynchronization scenario.

VI. EXPERIMENTAL RESULTS

We evaluate our proposed scheme on the Grizzly benchmark dataset described in [5]. Grizzly is based on leakage data collected from the data bus of the Atmel XMEGA 256 A3U, which is a widely used 8-bit micro-controller. While the use of data with 8-bit secrets may appear overly simplistic, it is well suited for the evaluation of the energy efficiency of countermeasures. Given the 8-bit nature of the system, there are 256 keys. For each key $k \in \{0, 1, \dots, 255\}$, 3072 raw traces are recorded. These traces are divided into two sets: a *profiling* set and an *attack* set. Each raw trace has 2500 samples, and each sample represents the total current consumption in all CPU ground pins.

The attack algorithm we used in the experiments is the linear model based Template Attack described in [9], [22]. In this attack, the leakage function is represented by a linear model (also called *stochastic model* in this context), and during profiling the leakage function and the model is estimated by solving the linear equations built from all or a subset of keys. Based on the estimated leakage function, the template, which typically is in form of Gaussian Model, for each key is built. In the attack phase, we select the candidate key with the maximum likelihood in matching. In our experiments, we use all keys (256 keys) for profiling the leakage function. As a baseline for key recovery, we also present the results of the original Template Attack (denoted by **OA**), which is the version without generating noise sequence injected into the raw traces.

The sampling methods that we used in the experiments include 3ppc, 20ppc, and allap, which are very typical compression methods in side-channel attacks. In the Grizzly dataset, the number of samples obtained by these methods in each trace typically are: 18 ~ 30 for 3ppc, 75 ~ 79 for 20ppc, and 125 for allap, respectively [8]. As we discussed in Section V, the chosen of the sampling method is based on the system's performance requirements, such as the security level and energy consumption budget. We will evaluate the different scenarios where the system and the attacker choose different sampling methods and discuss the principle of how to choose the appropriate sampling method for the specific system.

We compare our noise generation scheme to two other methods: Random Full Sequence and Random Partial Sequence. Random Full Sequence [12] generates random noise at all time. As a result, all leakage samples (in our experiments we have 2500 of them) are covered by random noise samples. Random Partial Sequence improves over Random Full Sequence by generating noise for adding onto only a randomly selected subset of the raw leakage samples. In order to fairly compare Random Partial Sequence to our scheme, we have both methods generate the same number $|\Omega_F|$ of noise samples. As a result, the two scheme only differ in the selection of raw leakage samples to inject the noise into. In the following, we use the term **ArN** to denote our proposed

artificial noise method, the terms **RnF** and **RnP** for Random Full Sequence and Random Partial Sequence, respectively.

A. Metrics and Settings

In the experiments, during the attack phase, for each key k , we independently run the attack 100 times by randomly picking the leakage traces from the *attacking* set. We use the *Successful_Recovery_Rate* (*SRR*) to measure the attack performance, which is the average success probability over **all** keys:

$$\text{Successful_Recovery_Rate} = \frac{\sum_{k=0}^{2^B-1} P_{\text{attack}}(k)}{2^B},$$

where $P_{\text{attack}}(k) = \frac{N_{\text{hit}}(k)}{N_T}$. Here N_T is the number of tests (in our case, $N_T=100$) and $N_{\text{hit}}(k)$ stands for how many times that key k is successfully guessed during all N_T tests. In the following, we will present which noise generation method most efficiently decreases the key recovery rate.

We defined the EE for an attack in Eq. (35). In our experiments, we use EE_{avg} to measure the average energy efficiency of the noise generation for **all** keys, and we define it as:

$$EE_{\text{avg}} = \frac{\sum_{k=0}^{2^B-1} \frac{\sum_{t=1}^{N_T} EE(k,t)}{N_T}}{2^B},$$

where $EE(k,t)$ is the *EE* value for an attack on key k in t -th test. To scale the result, we normalize the *Noise_Energy* in Eq. (35) by letting

$$\text{Noise_Energy} = \frac{\text{Noise_Energy}}{N_T \cdot 2500 \cdot \sigma^2},$$

where σ is the variance of the generated noise sequence, and the constant 2500 is the number of sample per trace in our experiments.

In order to fairly compare all noise generation methods, both noise vector N_r and noise vector N_a are generated from the same distribution. The parameters of the noise distribution is obtained from the raw leakage trace: We collect the raw leakage traces under $k = 0$ and compute the mean and variance. We generate the i.i.d noise vector for all noise generation methods based on the obtained parameters.

During the system design phase, we use 1000 traces to compute the matrix P for any given compression method.

B. Experimental Data and Analysis

In the following, we use I_a and I_p to denote the number of profiling and attack traces for each key, respectively.

Fig. 4 show the results of the successful recovery rate and the average EE for different values of A . The number of attack traces I_a and the number of profiling traces I_p are all fixed to 500. Initially, we assume that both the system designer and the attacker choose same sampling method: 20ppc. We also fix the gain $\rho = 1$ to control the overhead of the generated noise sequences. As **OA** has no noise generator, and **RnF** always covers the full size of leakage trace, the value of A is irrelevant to them. Hence, we repeat the experiments $N_T \cdot T_A$ times where T_A is the number of different A , and then take

the average. Finally, we get the constant values of *SRR* and *EE_{avg}* for **OA** and **RnF** under different A : the *SRRs* of **OA** and **RnF** are 91.64% and 44.43%, and the *EE_{avg}* of **RnF** is 0.094. Note that EE has no meaning for **OA**.

The results indicate that for a small numbers of A (such as < 50), **ArN** gets a better recovery rate (i.e., is less effective) compared to **RnF**. This is because now we can only get a partial solution of F from Eq. (34). When $A \geq 75$, which is also the lower bound of the number of samples by 20ppc, **ArN** can get the full or approximate full solution of F . As a result, **ArN** achieve full effectiveness, which is also verified from the experimental results that now both **ArN** and **RnF** allow for almost the same recovery rates. However, if we observe the EE values, we can clearly find that **ArN** always displays good EE value. This result proves that to achieve *same level* of security, our method has the benefits in spending much less energy compared to the **RnF**. For example, when $A \geq 70$, the EE values of **ArN** get to stay in around of 3.2, which is much better than **RnF**.

Actually, the effectiveness (resistance) of **RnP** is always the worst compared to other two noise generation methods. As both **RnP** and **ArN** generate the same number of noise samples, it's straightforward that **RnP**'s EE values are always worse than **ArN**'s. This also shows that the effectiveness of our proposed model relies on the fact that the generation of the noise samples is artificially designed and particularly target on the useful leakage samples. We also note that it is meaningless to compare the EE values of **RnF** and **RnP**, since they don't have a same or an approximate value in either the energy cost or the recovery rate.

Fig. 5 shows the recovery rates and EE values with different numbers of I_a . Here I_p remains 500, and I_a varies from 1 to 1000. We still assume that both the designer and attacker choose 20ppc as the sampling method. The value of A is set to 100, which allows for F to obtain the full solution. We also compare the effect of the gain: We show the results for gain $\rho = 1$ for all the noise generation methods, and we compare this to the use of increased gain $\rho = 2$ for **ArN** and **RnP** (now $E'_A = 4E_A$). With increasing numbers of attack traces, the recovery rate of the original Template Attack, and also of all the noise generation methods, increases. This is because the noise can be eliminated when a large number of traces is collected and averaged. However, when $\rho = 1$, even in the case of $I_a=1000$, **ArN** can still decrease the recovery rate from 95% (the Template Attack's number) to 55.27%, which is significant. At the same time, **ArN** also has the maximum average EE value, around 2.47, compared to other two noise generation methods. Still, this is also another good proof that compared to **RnF**, even under the same design on the noise's amplitude (the gain), our method can always spend much less energy, in order to get the same security level.

If now we increase the gain factor ρ to 2, in $I_a=1000$, **ArN** can even decrease the recovery rate to 31.52% with average EE of 0.9587, which is about 12.5 times better than the EE value of **RnF** (0.0766) when $\rho = 1$, and about 1.74 times better than the EE value of **RnP** (0.5508) when $\rho = 2$, but the recovery rate for both of these two methods are lager than **ArN**, with at least 20% increase. This also shows a fact that

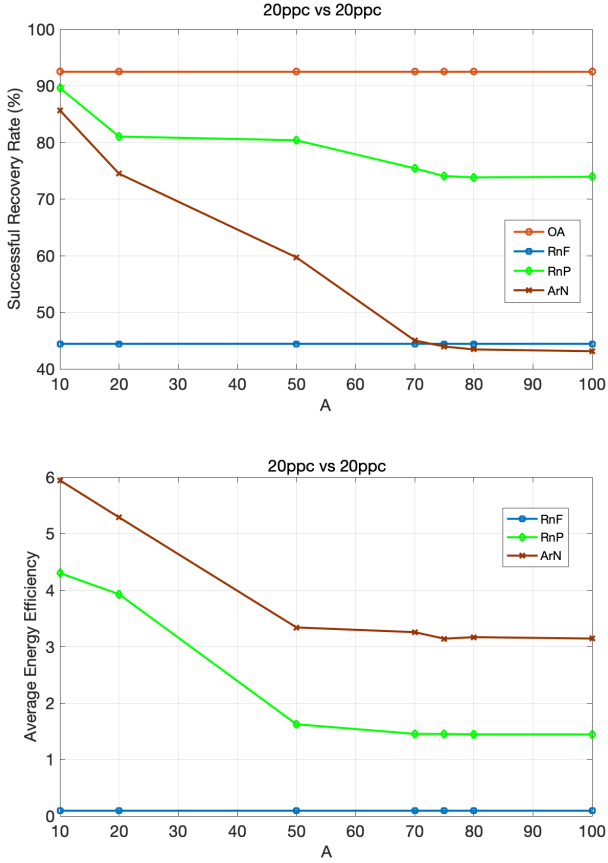


Fig. 4: Probability of Successful Recovery, and Average EE, versus Different A , with a Same Sampling Method 20ppc for System and Attacker

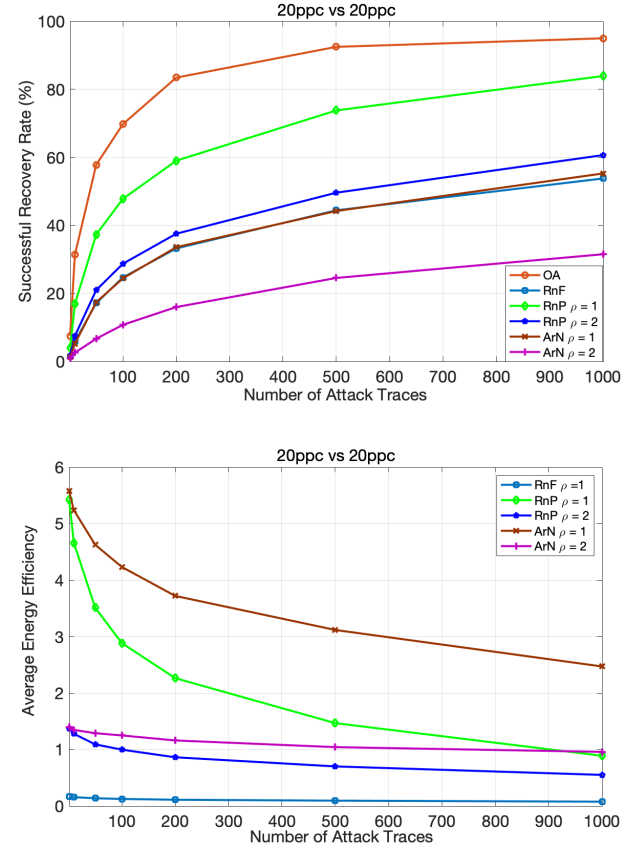


Fig. 5: Probability of Successful Recovery, and Average EE, versus Different Attack Traces I_a , with a Same Sampling Method 20ppc for System and Attacker

compared to **RnF**, **ArN** can generate the noise sequence to strongly enhance the security level on the system, but with much less energy to be spent. In general, the experimental data proves the significant energy efficiency of our method.

Naturally, the attacker will unlikely select the same compression method that the system designer consider for designing the noise sequence. As a case study, we want to analyze which sampling method is most suitable that used in system design for generating the artificial noise samples on the Atmel XMEGA 256 micro-controller (which is the platform that Grizzly dataset is collected from) for countering side-channel attacks. Tab. I shows the effects of the attacker choosing different selection methods than what the designer had in mind by comparing the recovery rates and EE values for all possible combinations of compression methods selected by the designer and attacker. We still fix I_p and I_a to be 500. The value of A is set to 150 hence the full solution of F can be guaranteed under any sampling method. The gain ρ is set to 1. Here S_D and S_A stand for the sampling method that is chosen by system designer and the attacker, respectively. We should note that, as no noise sequence is generated under **OA** and **RnF** is not affected by the sampling methods chosen by the designer, their recovery rates and EE values only differ for different attacker's sampling methods.

From the table, we can find that for the case that the attacker chooses 3ppc, **ArN** always has lower recovery rates compared to other sampling methods. This is a reasonable result since only a very limited leakage samples are picked under 3ppc. In general, no matter which defending methods is applied, the attacker will always get a lower recovery rate by using 3ppc compared to the other two sampling methods, which makes 3ppc a poor choice for the attacker in practice. If we look at the cases of (3ppc, 20ppc) and (3ppc, allap), **ArN** experiences much higher recovery rates compared to **RnF**. Hence, $S_D = 3ppc$ is a poor choice for the system designer as well, even if it brings huge saving in energy cost. In the case where the system designer selects allap as S_D , we find that for most of the time, the recovery rates of **ArN** are lower compared to the cases of other sampling methods are chosen as S_D , under same S_A . For example, when under (allap, allap), the recovery rate of **ArN** is only 42.25%. But the recovery rate becomes 54.32% when under (20ppc, allap). However, if we check the EE values, we find that for any fixed attacker's sampling method S_A , using 20ppc as S_D in defending is always more energy-efficient than using allap. For example, we have 3.1175 in (20ppc, 20ppc) and 1.8543 in (allap, 20ppc). Similarly, we get 2.3541 in (20ppc, allap) and 1.9148 in (allap, allap). We also mentioned that the recovery rate for **ArN** in (20ppc, allap) is about 12%

higher than in (allap, allap), but it's noticed that 54.32% is also not an unacceptable number, especially compared to **RnP** in the same case (73.18%). Hence, from this table, considering both the energy efficiency and the practicability in application, we recommend 20ppc as the *first choice* in the system design for the Grizzly dataset. In practice, if we need to design the artificial noise generator for other systems, we recommend that the designers also compute a similar table as Tab. I, and then select the sampling method based on the comparison of the values of both the effectiveness and the efficiency in each different (S_D, S_A) combinations, under the specific system's requirements, such as the energy consumption budget, gain, etc.

VII. CONCLUSION

In this paper, we propose an energy efficient scheme to generate artificial noise sequences to prevent side-channel attacks on devices. By mapping the side-channel attacks model to the communication model, we use channel capacity to measure the mutual information between the side-channel leakage and the secret, and hence map the optimal noise sequence design problem to a side-channel's channel capacity minimization problem. Different from previous random noise generation, we exploit the sparsity of the raw leakage traces that only a few number of leakage samples contain the useful leakage information. Finally, we provide the solution for generating the optimal noise sequence under a given energy constraint. Experimental results are also provided to show the effectiveness of our proposed scheme.

We see two directions for future work: First, the likely delay introduced by the noise generation hardware may give rise to *asynchronization*, where the generated noise sequence may not be exactly match with the leakage trace. In this paper, we assume that the cryptographic engine and the noise generator are in sync. Hence, the solution in Eq. (34) can be viewed as a theoretical bound for the artificial noise generation model. Second, we have limited the scope of compression methods to *sample selection* methods. We are currently investigating how these noise generation schemes fare against other compression methods, such as PCA and similar linear combination schemes, as well as optimal noise generation against these methods.

REFERENCES

- [1] E. Brier, C. Clavier, and F. Olivier, "Correlation Power Analysis with a Leakage Model," in *International Workshop on Cryptographic Hardware and Embedded Systems (CHES'04)*. Springer, 2004, pp. 16–29.
- [2] K. Gandolfi, C. Moutrel, and F. Olivier, "Electromagnetic Analysis: Concrete Results," in *International Workshop on Cryptographic Hardware and Embedded Systems (CHES'01)*. Springer, 2001, pp. 251–261.
- [3] A. Faruque, M. Abdullah, S. R. Chhetri, A. Canedo, and J. Wan, "Acoustic Side-Channel Attacks on Additive Manufacturing Systems," in *Proceedings of the 7th International Conference on Cyber-Physical Systems (ICCPs'16)*. IEEE, 2016, pp. 1–10.
- [4] P. Kocher, J. Jaffe, and B. Jun, "Differential Power Analysis," in *Advances in cryptology (CRYPTO'99)*. Springer, 1999, pp. 789–789.
- [5] Grizzly, "http://www.cl.cam.ac.uk/research/security/datasets/grizzly/."
- [6] J. Doget, E. Prouff, M. Rivain, and F.-X. Standaert, "Univariate Side Channel Attacks and Leakage Modeling," *Journal of Cryptographic Engineering*, vol. 1, no. 2, pp. 123–144, 2011.
- [7] S. Chari, J. R. Rao, and P. Rohatgi, "Template Attacks," in *International Workshop on Cryptographic Hardware and Embedded Systems (CHES'03)*. Springer, 2003, pp. 13–28.
- [8] M. O. Choudary and M. G. Kuhn, "Efficient template attacks," in *International Conference on Smart Card Research and Advanced Applications (CARDIS'13)*. Springer, 2013, pp. 253–270.
- [9] W. Schindler, K. Lemke, and C. Paar, "A Stochastic Model for Differential Side Channel Cryptanalysis," in *International Workshop on Cryptographic Hardware and Embedded Systems (CHES'05)*. Springer, 2005, pp. 30–46.
- [10] M. Rivain, "On the Exact Success Rate of Side Channel Analysis in the Gaussian Model," in *The 15th Annual Conference on Selected Areas in Cryptography (SAC'08)*. Springer, 2008, pp. 165–183.
- [11] E. Prouff and M. Rivain, "Masking against side-channel attacks: A formal security proof," in *32nd Annual International Conference on the Theory and Applications of Cryptographic Techniques (Eurocrypt'13)*. Springer, 2013, pp. 142–159.
- [12] A. Shamir, "Protecting smart cards from passive power analysis with detached power supplies," in *International Workshop on Cryptographic Hardware and Embedded Systems (CHES'00)*. Springer, 2000, pp. 1–77.
- [13] R. Poussier, Q. Guo, F.-X. Standaert, C. Carlet, and S. Guilley, "Connecting and improving direct sum masking and inner product masking," in *International Conference on Smart Card Research and Advanced Applications (CARDIS'18)*. Springer, 2018, pp. 123–141.
- [14] T. De Cnudde, O. Reparaz, B. Bilgin, S. Nikova, V. Nikov, and V. Rijmen, "Masking aes with $\$d+1\$$ shares in hardware," in *International Conference on Cryptographic Hardware and Embedded Systems (CHES'16)*. Springer Berlin Heidelberg, 2016, pp. 194–212.
- [15] D. Das, S. Maity, S. B. Nasir, S. Ghosh, A. Raychowdhury, and S. Sen, "High efficiency power side-channel attack immunity using noise injection in attenuated signature domain," in *2017 IEEE International Symposium on Hardware Oriented Security and Trust (HOST'17)*, 2017, pp. 62–67.
- [16] W. Yu, O. A. Uzun, and S. Köse, "Leveraging on-chip voltage regulators as a countermeasure against side-channel attacks," in *2015 52nd ACM/EDAC/IEEE Design Automation Conference (DAC'15)*, 2015, pp. 1–6.
- [17] M. Khan and Y. Chen, "A randomized switched-mode voltage regulation system for iot edge devices to defend against power analysis based side channel attacks," in *2021 IEEE International Conference on Big Data and Cloud Computing (BdCloud'21)*, 2021, pp. 1771–1776.
- [18] Q. Fang, L. Lin, Y. Z. Wong, H. Zhang, and M. Alioto, "Side-channel attack counteraction via machine learning-targeted power compensation for post-silicon hw security patching," in *2022 IEEE International Solid-State Circuits Conference (ISSCC'22)*, vol. 65, 2022, pp. 1–3.
- [19] S. Goel and R. Negi, "Guaranteeing secrecy using artificial noise," *IEEE Transactions on Wireless Communications*, vol. 7, no. 6, pp. 2180–2189, 2008.
- [20] F.-X. Standaert, T. Malkin, and M. Yung, "A Unified Framework for the Analysis of Side-Channel Key Recovery Attacks," in *28th Annual International Conference on the Theory and Applications of Cryptographic Techniques (Eurocrypt'09)*. Springer, 2009, pp. 443–461.
- [21] A. Heuser, O. Rioul, and S. Guilley, "Good is Not Good Enough: Deriving Optimal Distinguishers from Communication Theory," in *International Workshop on Cryptographic Hardware and Embedded Systems (CHES'14)*. Springer, 2014, pp. 55–74.
- [22] S. Jin and R. Bettati, "Adaptive Channel Estimation in Side Channel Attacks," in *2018 IEEE International Workshop on Information Forensics and Security (WIFS'18)*. IEEE, Dec 2018, pp. 1–7.
- [23] T. Unterluggauer, T. Korak, S. Mangard, R. Schilling, L. Benini, F. K. Gürkaynak, and M. Muehlberger, "Leakage bounds for gaussian side channels," in *International Conference on Smart Card Research and Advanced Applications (CARDIS'18)*. Springer, 2018, pp. 88–104.
- [24] T. M. Cover and J. A. Thomas, *Elements of Information Theory*. John Wiley & Sons, Inc., 2006.
- [25] A. Goldsmith, S. A. Jafar, N. Jindal, and S. Vishwanath, "Capacity limits of mimo channels," *IEEE Journal on Selected Areas in Communications*, vol. 21, no. 5, pp. 684–702, 2003.
- [26] R. Benadjila, E. Prouff, R. Strullu, E. Cagli, and C. Dumas, "Deep Learning for Side-Channel Analysis and Introduction to ASCAD Database," *Journal of Cryptographic Engineering*, vol. 10, pp. 163–188, 2020.
- [27] C. Sen, "Digital communications jamming," 2000.

(S_D, S_A) \ Methods	OA	RnF		RnP		ArN	
	SRR (%)	SRR (%)	EE_{avg}	SRR (%)	EE_{avg}	SRR (%)	EE_{avg}
(3ppc, 3ppc)	87.35	30.29	0.1154	76.14	5.4944	32.06	15.6425
(20ppc, 3ppc)	-	-	-	58.05	2.318	31.55	3.8385
(allap, 3ppc)	-	-	-	49.93	1.6603	33.43	2.2072
(3ppc, 20ppc)	92.49	44.43	0.094	88.76	2.5879	87.54	2.869
(20ppc, 20ppc)	-	-	-	73.8	1.4675	44.22	3.1175
(allap, 20ppc)	-	-	-	65.15	1.1555	44.08	1.8543
(3ppc, allap)	91.64	42.88	0.0947	86.8	3.0385	84.86	3.4856
(20ppc, allap)	-	-	-	73.18	1.4822	54.32	2.3541
(allap, allap)	-	-	-	64.7	1.1702	42.25	1.9148

TABLE I: Probability of Successful Recovery, and Average EE, versus Different Combinations of Sampling Methods for System Designer and Attacker

- [28] S. Shafiee and S. Ulukus, "Capacity of multiple access channels with correlated jamming," in *2005 IEEE Military Communications Conference (MILCOM'05)*, vol. 1, 2005, pp. 218–224.
- [29] T. Güneysu and A. Moradi, "Generic side-channel countermeasures for reconfigurable devices," in *International Workshop on Cryptographic Hardware and Embedded Systems (CHES'11)*. Springer, 2011, pp. 33–48.
- [30] C. Archambeau, E. Peeters, F.-X. Standaert, and J.-J. Quisquater, "Template Attacks in Principal Subspaces," in *International Workshop on Cryptographic Hardware and Embedded Systems (CHES'06)*. Springer, 2006, pp. 1–14.
- [31] B. Gierlichs, K. Lemke-Rust, and C. Paar, "Templates vs. Stochastic Methods," in *International Workshop on Cryptographic Hardware and Embedded Systems (CHES'06)*. Springer, 2006, pp. 15–29.
- [32] S. Mangard, E. Oswald, and T. Popp, *Power Analysis Attacks: Revealing the Secrets of Smart Cards*. Springer, 2008.
- [33] I. Mann, S. McLaughlin, W. Henkel, R. Kirkby, and T. Kessler, "Impulse generation with appropriate amplitude, length, inter-arrival, and spectral characteristics," *IEEE Journal on Selected Areas in Communications*, vol. 20, no. 5, pp. 901–912, 2002.
- [34] D. B. Levey and S. McLaughlin, "The statistical nature of impulse noise interarrival times in digital subscriber loop systems," *Signal Processing*, vol. 82, no. 3, pp. 329–351, 2002.